Heterogeneity of Tibial Plateau Cartilage in Response to a Physiological Compressive Strain Rate

Jessica M. Deneweth,[1,2] Kelly E. Newman,[1] Stephen M. Sylvia,[1] Scott G. McLean,[1] Ellen M. Arruda[2,3,4]

[1]School of Kinesiology, University of Michigan, Ann Arbor, Michigan 48109, [2]Department of Mechanical Engineering, University of Michigan, Ann Arbor, Michigan 48109, [3]Department of Biomedical Engineering, University of Michigan, Ann Arbor, Michigan 48109, [4]Program in Macromolecular Science and Engineering, University of Michigan, Ann Arbor, Michigan 48109

Received 10 April 2012; accepted 16 August 2012
Published online 5 September 2012 in Wiley Online Library (wileyonlinelibrary.com). DOI 10.1002/jor.22226

ABSTRACT: Knowledge of the extent to which tibial plateau cartilage displays non-uniform mechanical topography under physiologically relevant loading conditions is critical to evaluating the role of biomechanics in knee osteoarthritis. Cartilage explants from 21 tibial plateau sites of eight non-osteoarthritic female cadaveric knees (age: 41–54; BMI: 14–20) were tested in unconfined compression at 100% strain/s. The elastic tangent modulus at 10% strain ($E_{10\%}$) was calculated for each site and averaged over four geographic regions: not covered by meniscus (I); covered by meniscus—anterior (II); covered by meniscus—exterior (III); and covered by meniscus—posterior (IV). A repeated-measures mixed model analysis of variance was used to test for effects of plateau, region, and their interaction on $E_{10\%}$. Effect sizes were calculated for each region pair. $E_{10\%}$ was significantly different ($p < 0.05$) for all regional comparisons, except I–II and III–IV. The regional pattern of variation was consistent across individuals. Moderate to strong effect sizes were evident for regional comparisons other than I–II on the lateral side and III–IV on both sides. Healthy tibial cartilage exhibits significant mechanical heterogeneity that manifests in a common regional pattern across individuals. These findings provide a foundation for evaluating the biomechanical mechanisms of knee osteoarthritis. © 2012 Orthopaedic Research Society. Published by Wiley Periodicals, Inc. J Orthop Res 31:370–375, 2013

Keywords: cartilage; knee; mechanics; heterogeneity; osteoarthritis

Knee osteoarthritis (OA) has been suggested to develop via joint biomechanical mechanisms.[1–6] Altered knee biomechanics, due to injury or malalignment for example, may shift the cartilage contact pattern from regions well-adapted to specific loading patterns to regions poorly suited for such loads, inducing a deleterious cartilage stress state.[7–9] Recent research supports this tenet; individuals with increased anterior tibial translation following anterior cruciate ligament injury demonstrated strong signs of early cartilage degeneration.[10] A clear link between knee mechanics and OA initiation within the human joint, however, remains to be established.

Detailed knowledge of the mechanical response of healthy tibiofemoral joint articular cartilage (AC) is critical in ascertaining a direct link between abnormal knee mechanics and OA. While OA presents on both the tibial and femoral surfaces, the unique interplay between the tibial plateau and the overlaying menisci potentiates large AC mechanical variability[11] and provides a logical starting point for such an investigation. Tibial AC appears to exhibit inhomogeneity across its surface,[12–14] but the extent to which it manifests under physiological load states is largely unknown. The few studies[13,14] that provided detailed mapping of human tibial AC mechanics used measurement techniques that do not reflect the short loading periods (i.e., 15–300 ms) and high strain rates (i.e., 50–1,000%/s) experienced by knee AC in vivo.[15] Those that have examined AC mechanics under more physiologically relevant conditions did not provide detailed data for the entire tibial surface or included test specimens with OA.[11–13,16] The accuracy with which these findings can be extrapolated to model and interpret the response of the entire cartilage surface under in vivo loading conditions remains uncertain.

If biomechanical mechanisms of knee OA are to be successfully understood, then there is a critical need to assess tibial cartilage mechanics for non-osteoarthritic human tissue under physiological loading conditions, across the entire tibial surface, and with high spatial resolution. Additionally, if these data could be utilized to develop a universal template of AC mechanics, current in-vivo screening and treatment modalities designed to combat OA progression would be greatly enhanced by removing the need for subject-specific tissue properties. The purpose of this study, therefore, was threefold: (1) to map the physiological mechanical properties of healthy human tibial AC across the tibial plateau, (2) to determine if differences in AC mechanical properties are regionally dependent, and (3) to delineate whether regional variations in tibial AC mechanical properties are expressed consistently across specimens.

METHODS

Eight unpaired fresh-frozen Caucasian female cadaveric knees were obtained for this study (Table 1). Inclusion criteria were BMI less than 26 kg/m^2, age between 18 and 55, and no history of osteoarthritis, osteoporosis, or lower limb injury or surgery. Mean age ($\pm$ 1 SD) was 49 $\pm$ 4 years and mean BMI was 17 $\pm$ 2 kg/m^2. All knees were stored at -20°C and completely thawed overnight prior to dissection.

The authors report no conflicts of interest.
Grant sponsor: Rackham Graduate School, University of Michigan.

Correspondence to: Jessica M. Deneweth (T: 248-568-6369; F: 734-764-5237; E-mail: jmden@umich.edu)

Table 1. Knee Donor Demographics

Donor	Knee	Age	BMI	Cause of Death
1	Left	41	19	Cancer, brain
2	Left	52	20	Cancer, unspecified
3	Left	54	14	Cancer, small bowel
4	Right	51	19	Cancer, lung
5	Right	51	16	Cancer, lung
6	Right	49	14	Cancer, breast
7	Left	52	19	Cancer, appendix
8	Right	44	18	Neurofibrosarcoma

To obtain the AC explants, each knee was dissected to expose the tibial articular surface. The inner boundary of each meniscus was outlined on the cartilage surface with black India ink, indicating its position in the unloaded knee at 0° of knee flexion, and then removed. A 4 × 3 grid pattern was drawn onto each plateau using black India ink such that a maximum amount of the plateau fell under the grid. The typical grid cell measured five millimeters mediolateral by 8 mm anteroposterior. Full thickness cylindrical cartilage explants without subchondral bone were extracted from the center of 21 cells (Fig. 1) of the grids using a 4-mm diameter round-hole hand punch (McMaster-Carr, Elmhurst, IL) and a surgical scalpel.[17] Explants were not removed from regions of fibrillated cartilage, as identified by an India ink test.[18] Each explant was stored in phosphate buffered saline solution (PBS) at −20°C until testing,[19,20] which has been found to maintain the mechanical integrity of the tissue.[21]

The testing apparatus used in this study was a custom-built device designed for testing compliant materials at linear speeds up to 1,000 mm/s (Fig. 2). It consisted of a high-speed electric linear actuator (SMAC, Carlsbad, CA; positional accuracy: ± 0.001 mm), a dynamic load cell (Dytran Instruments, Chatsworth, CA; sensitivity: 120 mV/N), a high-speed video camera (Photron USA, San Diego, CA; maximum frame rate: 5,400 frames/sec), and a transparent acrylic PBS bath. The load cell was mounted at one end of the water bath such that its sensing surface faced inward and was perpendicular to the line of action of the actuator rod. The actuator traveled horizontally directly in line with the load cell and entered the bath through the opposite end. Compression plates (15.78-mm diam., Dytran Instruments)

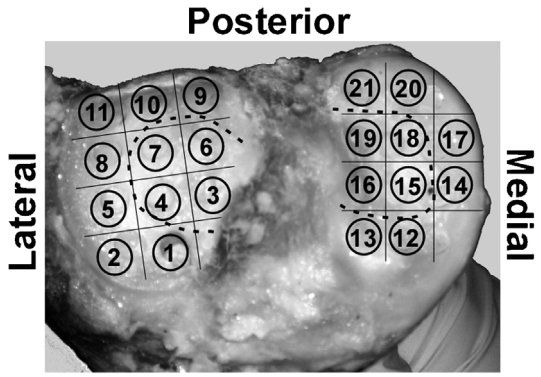

Figure 1. Numbered test sites on the tibial plateau from which AC explants were procured. Solid lines represent the applied grid pattern used to define the test sites. Dashed lines denote typical inner margins of the menisci.

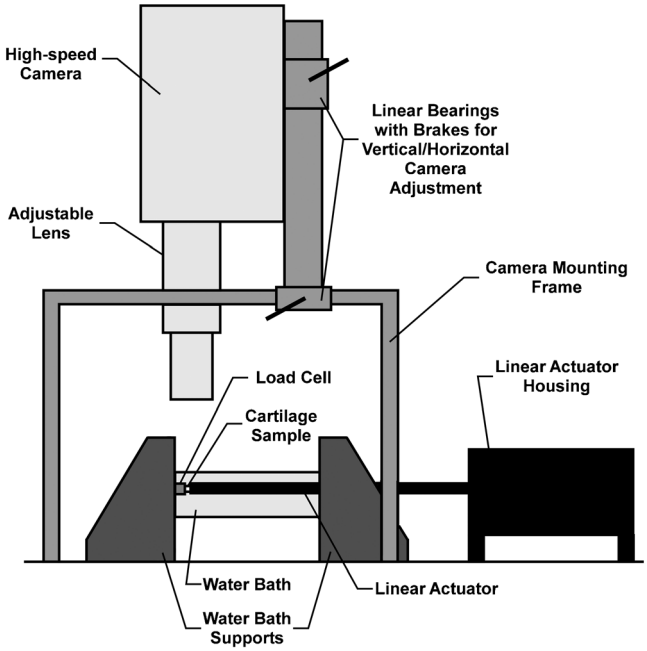

Figure 2. Schematic of the mechanical testing device used to test cartilage specimens in unconfined compression.

were attached to the facing ends of the load cell and the actuator rod. The camera was mounted over the water bath, and movements of the linear actuator were synced with force and camera data acquisition using a custom LabVIEW program (National Instruments, Austin, TX).

Diameter and thickness measurements were obtained using digital vernier calipers (resolution: 0.01 mm, Mitutoyo America Corporation, Aurora, IL) once the explant had completely thawed in the PBS bath. Sample thicknesses ranged from 0.9 to 4.4 mm. A speckle pattern was applied to the cylindrical surface of the cartilage sample using black India ink. The explant was situated between the force sensor and actuator rod under a minimal (0.2 N) tare load and allowed to equilibrate for 10 min.[22] To ensure a consistent tissue response, the explant was pre-conditioned with 10 cycles of loading at 100%/s to a peak strain of 20%. Three separate experimental trials of 100%/s compression to 20% peak strain and immediate return to 0% strain were subsequently conducted. Simultaneous force and video data were collected at 125 samples/s. Several minutes were allowed between trials for the specimen to re-equilibrate.

The average nominal strain along the thickness of the explant was calculated using commercial digital image correlation software (VIC-2D 2009, Correlated Solutions, Columbia, SC). This software tracks the deformations of the ink speckle pattern in each video frame and converts them to strain fields.[23] Nominal stress was calculated by dividing the recorded force by the undeformed cross-sectional area of the explant. Due to the nonlinear stress–strain relationship of AC and the strain-driven nature of this test, AC mechanics were quantified by the tangent modulus to the stress–strain curve at 10% strain ($E_{10\%}$). The mean and standard deviation of $E_{10\%}$ at each (n = 21) site was determined. Based on pilot data and published methods for quantifying regional variations in tibial geometry,[14,24] we hypothesized that the medial and lateral plateaus each could be divided into four explicit regions: not covered by meniscus; covered by meniscus—

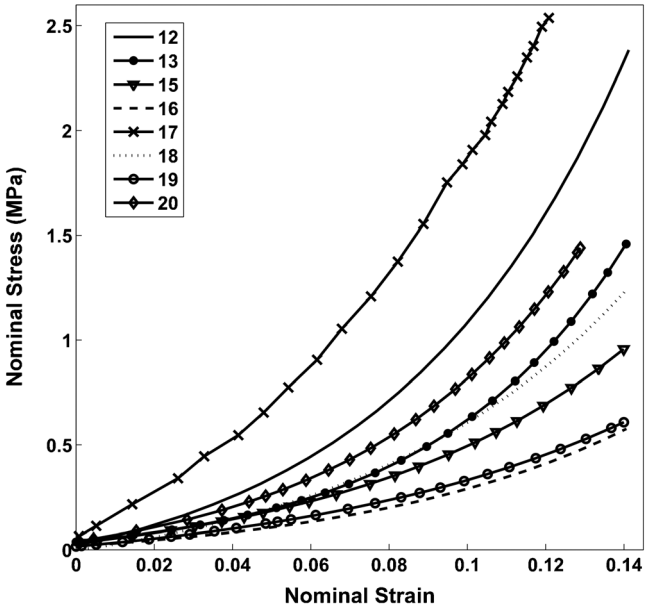

Figure 3. Sample stress–strain curve for eight AC explants taken from the same medial plateau. Under a strain rate of 100% strain/s, the explants demonstrated large differences in overall stiffness despite being from the same knee. The explants from meniscus-covered sites generally displayed steeper responses compared to sites not covered by meniscus.

anterior; covered by meniscus—exterior; and covered by meniscus—posterior. Therefore, the 21 test sites were grouped into these four regions (Fig. 4) and the region-based means and standard deviations of $E_{10\%}$ were calculated.

The mean regional values of $E_{10\%}$ were submitted to a repeated-measures mixed model analysis of variance to test for the effects of plateau (medial or lateral), region ($n = 4$), and the interaction of plateau × region ($n = 8$). Bonferroni-adjusted pairwise comparisons were made for all main effects. Significance was denoted by an alpha level of 0.05. The mixed model analysis was conducted using SAS 8.0 statistical software (SAS Institute Inc., Cary, NC). The effect size between two regions on the same plateau was evaluated using Cohen's d,[25] where $d_{AB} = \frac{\overline{E}_{10\%,B} - \overline{E}_{10\%,A}}{S_P}$ was the effect size between Regions A and B, $\overline{E}_{10\%,A}$ was the mean value of $E_{10\%}$ for Region A, $S_P = \sqrt{\frac{S_A{}^2(n_A-1)+S_B{}^2(n_B-1)}{n_A+n_B}}$ was the pooled standard deviation of Regions A and B, and n_A is the number of samples in Region A. The cut-off levels of d_{AB} for small, moderate, and strong effect sizes were 0.2, 0.5, and 0.8, respectively.

RESULTS

Of the 168 explants, 40 were excluded due to surface fibrillation identified by staining with India ink, damage incurred during extraction, or an inability to elicit peak strains greater than 10%. For the remaining explants, the stress–strain response under 100%/sec loading varied considerably (Figs. 3 and 4). Laterally, $E_{10\%}$ ranged from 4.69 MPa in the center of the plateau to 20.40 MPa on its posterior edge. Similarly for the medial plateau, $E_{10\%}$ ranged from 7.01 MPa in the center to 30.83 MPa at the posterior margin.

Mixed model analysis revealed that when the 21 sites were grouped into the four pre-defined regions

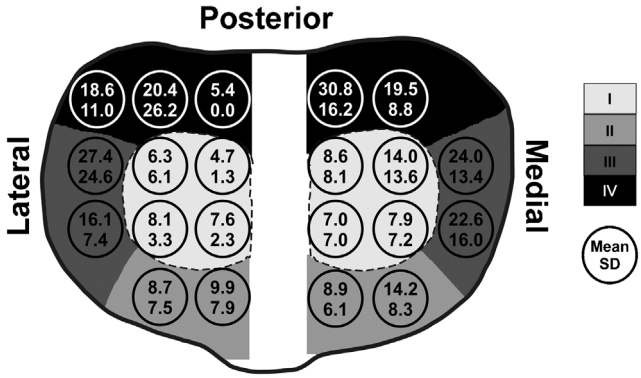

Figure 4. Mean and standard deviation of $E_{10\%}$ (MPa) across the tibial plateau. The gray scale mapping identifies the four regions into which the site data were grouped for statistical analysis. Dashed lines denote the inner margins of the menisci.

statistically significant differences in $E_{10\%}$ were evident (Fig. 5). Region I had a significantly lower value of $E_{10\%}$ compared to region III and region IV ($p < 0.001$ for both cases). Similarly, region II was significantly less stiff than regions III and IV ($p = 0.003$ and $p < 0.001$, respectively). No significant differences were present between regions I and II ($p = 1.00$) and regions III and IV ($p = 1.00$). Examining the effect sizes for these two comparisons (Table 2), the mean differences between III and IV were weak or small whereas between I and II the difference was moderate on the medial plateau and nearly moderate on the lateral plateau. There was no significant effect on $E_{10\%}$ due to medial or lateral plateau ($p = 0.245$).

In order to examine the consistency of the regional differences across knees, the regional patterns of $E_{10\%}$ in each of the eight knees tested were compared qualitatively. Since no statistically significant differences

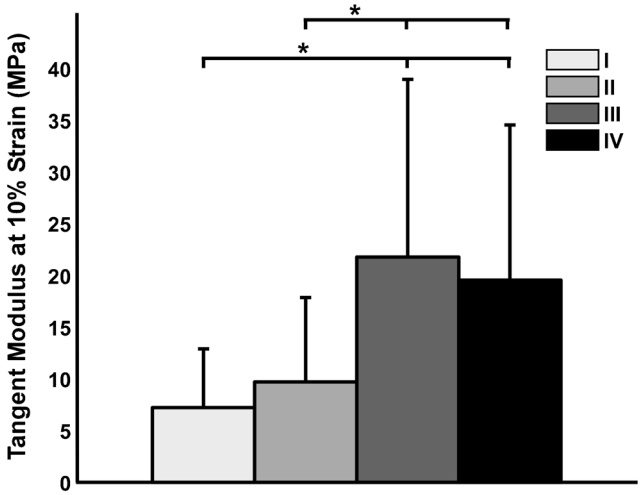

Figure 5. Mean $E_{10\%}$ (MPa) across the four pre-defined regions of the tibial plateau. Bars represent one standard deviation. Statistically significant ($p < 0.05$) differences between regions are indicated by *. Regions I and II were similar in magnitude and significantly less stiff than Regions III and IV, which did not differ significantly from each other.

Table 2. Mean, Sample Size (N), 95% Confidence Interval (CI), and Effect Size (d_{AB}) for Difference in $E_{10\%}$ (MPa) Between Regions

	I–II	I–III	I–IV	II–III	II–IV	III–IV
Lateral						
Mean	2.40	15.49	13.29	13.09	10.89	−2.20
N	33	33	31	30	28	28
95% CI	(−1.55, 6.36)	(6.53, 24.45)	(5.08, 21.49)	(2.73, 23.44)	(1.23, 20.54)	(−15.77, 11.37)
d_{AB}	0.43	1.23	1.21	0.95	0.88	0.13
Effect	Small	Strong	Strong	Strong	Strong	Weak
Medial						
Mean	4.04	15.49	18.79	11.46	14.75	3.29
N	38	41	43	25	27	30
95% CI	(−0.88, 8.96)	(9.14, 21.85)	(12.72, 24.85)	(1.93, 20.99)	(5.65, 23.85)	(−6.78, 13.37)
d_{AB}	0.60	1.62	1.97	1.00	1.31	0.24
Effect	Moderate	Strong	Strong	Strong	Strong	Small

were observed in $E_{10\%}$ between plateaus, data from both plateaus were averaged for this analysis (Fig. 6). A consistent pattern was evident across the eight knees, where regions I and II were similar to each other and substantially less stiff than regions III and IV, which were also similar to each other.

DISCUSSION

Characterizing the response of healthy tibial AC to physiological loading rates is critical to determining and counteracting the mechanism(s) of knee OA development and progression. This study uniquely addressed this need by quantifying the tissue's stress–strain response under a physiologically-relevant strain rate at 21 sites across eight non-osteoarthritic human-tibial plateaus. Study outcomes confirmed that tibial AC exhibits non-uniform, region-specific properties. Furthermore, these regional mechanical variations are consistent across knee specimens, indicating that they may represent universal trends for the study population.

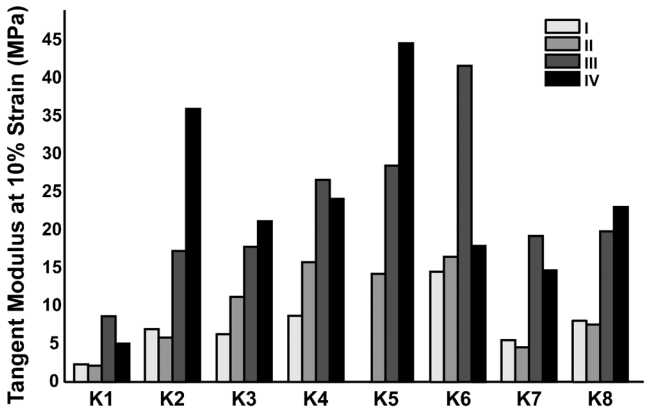

Figure 6. Mean $E_{10\%}$ (MPa) across the four pre-defined regions of the tibial plateau for each knee. *K1* indicates Knee 1. A consistent pattern is evident across all eight knees, with Regions I and II softer than Regions III and IV. No data is available for Region I of K5 due to compromised AC quality in that area of the plateau.

The loading parameters used (100% strain/s and 20% peak strain) were consistent with those recently observed for in-vivo AC deformation during the stance phase of gait.[15] AC displayed values of $E_{10\%}$ that ranged from 1.0–80.0 MPa, which agrees well with the work of previous authors.[11,13] Thus, the reported stress–strain behaviors reflected those likely to occur under true physiological loading conditions. The lateral and medial tibial plateaus were divided into 11 and 10 test sites, respectively, to ensure that the most locations could be consistently sampled on each plateau. A large variation in $E_{10\%}$ was evident across the surface, with the stiffest locations exhibiting $E_{10\%}$ nearly five times larger than $E_{10\%}$ at the most compliant sites.

Significant differences in $E_{10\%}$ were observed when averaged and compared across four respective regions of the medial and lateral plateaus. Reducing the 21 tibial surface sites into these regions afforded more tractable and clinically relevant inferences regarding relationships between cartilage contact patterns and tissue mechanics. For the medial and lateral plateaus, regions I (i.e., not covered by meniscus) and II (i.e., anterior third of the meniscus-covered area) consistently displayed the lowest average $E_{10\%}$. Regions III and IV (i.e., exterior and posterior meniscus-covered, respectively) were stiffer than I and II, but were minimally different from each other in terms of $E_{10\%}$. These findings suggest that much of the variability in the mechanical response of tibial AC can by adequately represented by three, rather than four, distinct regions, contrary to our initial hypothesis. These regions, listed in order of increasing stiffness, are: meniscus-uncovered, anterior meniscus-covered, and exterior-posterior meniscus-covered. This result indicates that significant variability exists not only between meniscus-covered and meniscus-uncovered regions but also within the meniscus-covered area.

The regional pattern of $E_{10\%}$ does not appear to be subject-specific in the study population. Additionally, the plateau (lateral or medial) from which the explant was taken did not contribute significantly to $E_{10\%}$.

Taken together, these findings suggest that the regional mapping presented herein could serve as a template for healthy tibial AC stiffness within this population.

The significant regional variations observed in the AC mechanical response to physiological loads provide new insights for a potential mechanism of OA development. During ambulatory gait, primary cartilage deformation typically occurs in the center of the plateau where the cartilage is not covered by meniscus (i.e., region I).[2,8] Since this region was the most compliant, it appears well-adapted to sustaining large deformations, such as at heel strike, without concomitant damage to the tissue structure. Adjacent test sites exhibited substantially different tangent elastic moduli, suggesting that a few-millimeter shift from the normal contact pattern may move primary loading to stiffer and perhaps less suitable regions (e.g., regions III and/or IV). Depending on concurrent changes in cartilage contact area and in the percentage of load borne by the menisci, similar magnitude deformations in these regions, which are three to four times stiffer than region I, could produce substantially larger stresses in the tissue. Several studies have shown that knees with a surgically reconstructed anterior cruciate ligament display increased anterior tibial laxity and external tibial rotation during demanding functional tasks compared to their uninjured contralateral knee or healthy control knees.[26–28] These altered joint kinematics could shift primary knee joint contact to stiffer, less optimal tibial AC regions.[10,29,30] Further research is needed to determine, given the findings of the present study, whether such kinematic changes identified in vivo can indeed promote OA development. Additionally, as OA lesions are also highly prevalent on the femur[31] work must be done to characterize the mechanical variability of femoral cartilage. Our group is currently undertaking this research.

Several factors should be considered when interpreting the results of this study. First, the AC mechanical response was characterized using a single parameter, $E_{10\%}$, to afford comparison with previous literature. This parameter, while insightful, does not fully capture the mechanics of non-linear tissue. A more comprehensive data analysis using non-linear analytical models is forthcoming.[32] Second, the menisci are known to translate as much as 10 mm posteriorly over the tibia during knee flexion.[33] Thus, some of the cartilage sites may experience both meniscus-uncovered and meniscus-covered loading during the course of the gait cycle rather than the single type of loading that their regional (I–IV) characterization suggests. This may explain some of the variability found in $E_{10\%}$within each region. Third, as AC is a viscoelastic tissue with strain rate dependent properties,[34] extrapolation of these findings to describe the response of cartilage under higher rate loading, such as during running or jumping, must be done with caution. Finally, the applicability of these results to the general population is limited. The sex, race, age, and knee health of the donors for this study were tightly controlled to reduce inter-subject variability. Additionally, the specimens' BMIs were lower than the average population, and activity level and limb alignment information were not available.

In conclusion, a mapping of the mechanical response of healthy female tibial AC to physiological compressive loading was completed. The tangent modulus at 10% strain was found to be significantly non-uniform across the tibial plateau. The heterogeneity of AC was successfully characterized across specimens by three topographic regions that demonstrate different mean elastic tangent moduli. Within this mapping, the external-posterior portion of the plateau was significantly stiffer than the adjacent regions, lending insight into the tenet that altered joint contact patterns play a critical role in the knee OA mechanism. Future work will focus on examining this interaction between joint contact patterns and the underlying cartilage morphology, as well as extending analyses to the femoral and male AC and employing non-linear parameters to model the AC response.

ACKNOWLEDGMENTS

The authors gratefully acknowledge Mr. Harish Iyer and Mr. Kevin Lapprich for their technical assistance, Mr. Ken Guire for his invaluable help with statistical analyses, and Anatomy Gifts Registry, Inc. and MedCure, Inc. for providing the knees used in this study. Ms. Deneweth is supported by the Department of Defense through a National Defense Science and Engineering Graduate Fellowship. This research was funded in part through a grant from the Rackham Graduate School of the University of Michigan.

REFERENCES

1. Andriacchi TP, Mundermann A, Smith RL, et al. 2004. A framework for the in vivo pathomechanics of osteoarthritis at the knee. Ann Biomed Eng 32:447–457.
2. Andriacchi TP, Koo S, Scanlan SF. 2009. Gait mechanics influence healthy cartilage morphology and osteoarthritis of the knee. J Bone Joint Surg Am 91:95–101.
3. Astephen JL, Deluzio KJ, Caldwell GE, et al. 2008. Gait and neuromuscular pattern changes are associated with differences in knee osteoarthritis severity levels. J Biomech 41:868–876.
4. Fleming BC, Hulstyn MJ, Oksendahl HL, et al. 2005. Ligament injury, reconstruction and osteoarthritis. Curr Opin Orthop 16:354–362.
5. Ristanis S, Giakas G, Papageorgiou CD, et al. 2003. The effects of anterior cruciate ligament reconstruction on tibial rotation during pivoting after descending stairs. Knee Surg Sports Traumatol Arthrosc 11:360–365.
6. Sharma L, Song J, Felson DT, et al. 2001. The role of knee alignment in disease progression and functional decline in knee osteoarthritis. JAMA 286:188–195.
7. Chaudhari AM, Briant PL, Bevill SL, et al. 2008. Knee kinematics, cartilage morphology, and osteoarthritis after ACL injury. Med Sci Sports Exerc 40:215–222.
8. Carter DR, Beaupre GS, Wong M, et al. 2004. The mechanobiology of articular cartilage development and degeneration. Clin Orthop Relat Res 462:S69–S77.
9. Andriacchi TP, Briant PL, Bevill SL, et al. 2006. Rotational changes at the knee after ACL injury cause cartilage thinning. Clin Orthop Relat Res 464:39–44.

10. Haughom B, Schairer W, Souza RB, et al. 2012. Abnormal tibiofemoral kinematics following ACL reconstruction are associated with early cartilage matrix degeneration measured by MRI T1 rho. Knee 19:482–487.
11. Shepherd DE, Seedhom BB. 1999. The 'instantaneous' compressive modulus of human articular cartilage in joints of the lower limb. Rheumatology (Oxford) 38:124–132.
12. Thambyah A, Nather A, Goh J. 2006. Mechanical properties of articular cartilage covered by the meniscus. Osteoarthritis Cartilage 14:580–588.
13. Young AA, Appleyard RC, Smith MM, et al. 2007. Dynamic biomechanics correlate with histopathology in human tibial cartilage: a preliminary study. Clin Orthop Relat Res 462: 212–220.
14. Swann AC, Seedhom BB. 1993. The stiffness of normal articular cartilage and the predominant acting stress levels: implications for the aetiology of osteoarthrosis. Br J Rheumatol 32:16–25.
15. Liu F, Kozanek M, Hosseini A, et al. 2010. In vivo tibiofemoral cartilage deformation during the stance phase of gait. J Biomech 43:658–665.
16. Barker MK, Seedhom BB. 2001. The relationship of the compressive modulus of articular cartilage with its deformation response to cyclic loading: does cartilage optimize its modulus so as to minimize the strains arising in it due to the prevalent loading regime? Rheumatology (Oxford) 40:274–284.
17. Lewis RJ, MacFarland AK, Anandavijayan S, et al. 1998. Material properties and biosynthetic activity of articular cartilage from the bovine carpo-metacarpal joint. Osteoarthritis Cartilage 6:383–392.
18. Meachim G. 1972. Light microscopy of Indian ink preparations of fibrillated cartilage. Ann Rheum Dis 31:457–464.
19. Krishnan R, Park S, Eckstein F, et al. 2003. Inhomogeneous cartilage properties enhance superficial interstitial fluid support and frictional properties, but do not provide a homogeneous state of stress. J Biomech Eng 125:569–577.
20. Ronken S, Arnold MP, Ardura Garcia H, et al. 2012. A comparison of healthy human and swine articular cartilage dynamic indentation mechanics. Biomech Model Mechanobiol 11:631–639.
21. Szarko M, Muldrew K, Bertram JE. 2010. Freeze-thaw treatment effects on the dynamic mechanical properties of articular cartilage. BMC Musculoskelet Disord 11:231.
22. Jurvelin JS, Buschmann MD, Hunziker EB. 2003. Mechanical anisotropy of the human knee articular cartilage in compression. Proc Inst Mech Eng H 217:215–219.
23. Ma J, Smietana MJ, Kostrominova TY, et al. 2012. Three-dimensional engineered bone-ligament-bone constructs for anterior cruciate ligament replacement. Tissue Eng A 18: 103–116.
24. Eckstein F, Wirth W, Hudelmaier M, et al. 2008. Patterns of femorotibial cartilage loss in knees with neutral, varus, and valgus alignment. Arthritis Rheum 59:1563–1570.
25. Cohen J. 1988. Statistical power analysis for the behavioral sciences. Hillsdale, NJ: L. Erlbaum Associates.
26. Deneweth JM, Bey MJ, McLean SG, et al. 2010. Tibiofemoral joint kinematics of the ACL-reconstructed knee during a single-leg hop landing. Am J Sports Med 38:1820–1828.
27. Almekinders LC, Pandarinath R, Rahusen FT. 2004. Knee stability following anterior cruciate ligament rupture and surgery. The contribution of irreducible tibial subluxation. J Bone Joint Surg Am 86-A:983–987.
28. Tashman S, Kolowich P, Collon D, et al. 2007. Dynamic function of the ACL-reconstructed knee during running. Clin Orthop Relat Res 465:66–73.
29. Salmon LJ, Russell VJ, Refshauge K, et al. 2006. Long-term outcome of endoscopic anterior cruciate ligament reconstruction with patellar tendon autograft: minimum 13-year review. Am J Sports Med 34:721–732.
30. Oiestad BE, Holm I, Aune AK, et al. 2010. Knee function and prevalence of knee osteoarthritis after anterior cruciate ligament reconstruction: a prospective study with 10 to 15 years of follow-up. Am J Sports Med 38:2201–2210.
31. Wirth W, Hellio Le Graverand MP, Wyman BT, et al. 2009. Regional analysis of femorotibial cartilage loss in a subsample from the Osteoarthritis Initiative progression subcohort. Osteoarthritis Cartilage 17:291–297.
32. Deneweth JM, Pomeroy S, Sylvia SM, et al. In Progress. Comparison of non-linear network models for modeling proximal tibial cartilage under physiological strain rates.
33. Thompson WO, Thaete FL, Fu FH, et al. 1991. Tibial meniscal dynamics using three-dimensional reconstruction of magnetic resonance images. Am J Sports Med 19:210–215; discussion 215–216.
34. Oloyede A, Flachsmann R, Broom ND. 1992. The dramatic influence of loading velocity on the compressive response of articular cartilage. Connect Tissue Res 27:211–224.